# Frequency-dependent interface capacitance of $Al-Al_2O_3-Al$ tunnel junctions

K. T. McCarthy, S. B. Arnason, and A. F. Hebard[a)]
*Department of Physics, University of Florida, Gainesville, Florida 32611-8440*

(Received 6 August 1998; accepted for publication 13 November 1998)

Four-terminal ac impedance measurements have been used to characterize $Al-Al_2O_3-Al$ tunnel-junction capacitors over the frequency range of 10 Hz–100 kHz. The insulating barriers are thin enough to assure that the response can be modeled by a frequency-dependent interface capacitance in parallel with a frequency-independent tunnel junction resistor $R_0$. The data reveal no sign of loss peaks down to 10 Hz and the impedance curves for a single junction, annealed to give different tunnel-junction resistance, collapse onto a single curve when $R_0$ is used as a scaling parameter. The loss mechanism is ascribed to interface traps and is found to give an unusual asymptotic phase angle response when the real and imaginary parts of the complex capacitance are plotted against each other. © *1999 American Institute of Physics.* [S0003-6951(99)05002-0]

The limitations on how a tunnel junction can be used in a chosen application depend on a full understanding of the electronic processes associated with the metal/dielectric interfaces defining the tunnel-junction barrier. A useful starting point for such an understanding is the realization that the capacitance is not simply the geometrical capacitance but also includes a contribution from interface processes that give rise to additional voltage drops at the interfaces of each electrode. Evidence that such processes are significant in the limit of small electrode separation can be found in studies of metal–insulator–metal (MIM) structures for a variety of metals (M=Au, Bi, Ta, Al, Pt) and insulators ($I=Ta_2O_5$, $Al_2O_3$, ZnS, $Ba_{0.5}Sr_{0.5}Ti0_3$).[1–4] In all of these works the measured capacitance $C_m$, is modeled as a series combination of a geometric bulk capacitance $C_g$, and an interface capacitance $C_i$. The applicability of this model (i.e., $C_m^{-1}=C_i^{-1}+C_g^{-1}$) is confirmed by a linear dependence of $C_m^{-1}$ on electrode separation $d$, where the reciprocal of the $y$ intercept at $d=0$ determines $C_i$ and the $x$ intercept at $d=-d_0$ determines the plate separation $d_0$ where $C_i=C_g$. For $Al-Al_2O_3-Al$ capacitors, previous experimental measurements have verified the linear dependence of $C_m^{-1}$ on $d$ and found $C_i=1.6\ \mu F/cm^2$ and $d_0=50$ Å.[3]

An insight into the origin of the large value for $d_0$ is found in a theoretical analysis which solves for the screened electrostatic potential in an $Al-Al_2O_3-Al$ trilayer structure.[5] A schematic of the spatial dependence of the electrostatic potential divided by areal charge density is shown in the inset of Fig. 1. The potential drop across the bulk of the dielectric is linear as expected, but there is also a significant drop across the two interfaces. This drop across the interfaces derives from a combination of two effects: the screening of charge in the metal and the redistribution of charge at the dielectric interface. As $d\rightarrow 0$ the total capacitance becomes the interfacial capacitance with an effective thickness of $d_0$ ($d_0/2$ from each interface). For $Al-Al_2O_3-Al$ capacitors, $d_0$ is calculated from the theory to be 19 Å,[5] a value more than a factor of 2 less than the experimentally determined value of 50 Å.[3] The discrepancy is most likely due to additional diffuse scattering associated with surface roughness and the presence of electron traps at the interfaces.

In this letter we present a study of the complex frequency-dependent impedance $Z(\omega)$ of $Al-Al_2O_3-Al$ tunnel junctions which have a thickness $d$ on the order of 20 Å and, hence, since $d<d_0$, a capacitance that is dominated by the potential drop across the two interfaces. This is an especially interesting regime since the presence of tunneling electrons associated with the small electrode separation should have a strong influence on the interface properties. Our impedance measurements confirm this suspicion and reveal a pronounced frequency dependence to the interface capacitance that is affected by the dc tunnel-junction resistance $R_0$. We attribute the frequency dependence to interface traps which when filled give rise to dissipation and capacitance changes.[6] There is no evidence of a loss peak in any of our tunnel junctions at frequencies as low as 10 Hz. Interest-

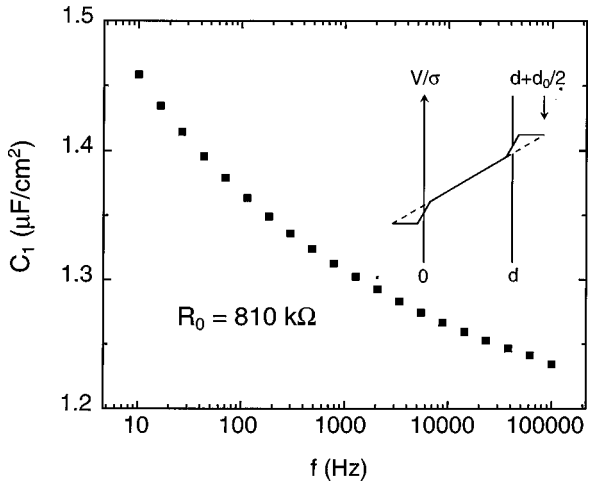


FIG. 1. Frequency dependence of the real part $C_1$ of the areal capacitance for a tunnel-junction capacitor with dc tunnel-junction resistance $R_0=850$ kΩ. The inset shows schematically how the voltage (normalized to surface charge density) varies across the metal electrodes separated by a dielectric of thickness $d$.

a)Electronic mail: afh@phys.ufl.edu

 

ingly, when a given tunnel junction is annealed by room-temperature aging, the resulting changes in $R_0$ and $C_i$ are well described by the collapse of all the impedance data onto a single curve when $R_0$ is used as a scaling parameter. A Cole–Cole plot of the complex capacitance reveals that the imaginary part of the capacitance is strongly reduced with increasing $R_0$ and asymptotically approaches zero in the high-frequency limit.

The tunnel junctions for this study were made by freshly evaporating Al through a shadow mask at a pressure of $5\times10^{-7}$ Torr. Base electrodes were then oxidized without breaking vacuum in a dc glow discharge at a partial oxygen pressure of 50 mTorr. Typical oxidation times ranged from 10 s to 3 min so that a variety of tunnel-junction samples with resistance values ranging from 100 Ω to 100 MΩ could be obtained. A mask with five equally spaced counterelectrode stripes was used for the counterelectrode deposition. The areas of all the junctions were nominally the same ($8.9\times10^{-3}$ cm$^2$) and there was very little variation in the resistance and capacitance of the five junctions fabricated in a given run. Fortunately, for the purposes of this study, the junctions aged over a period of weeks in laboratory air, giving rise to an increased $R_0$ and a changed capacitance. As shown below, this process allowed a comparison of the electrical response in the same structure with continuously varying tunnel barrier parameters.

Measurements of the complex impedance were made in a four-terminal configuration using phase sensitive detection over the frequency range $10-10^5$ Hz. Shown in Fig. 1 is a plot of the real part of the areal capacitance versus frequency for a tunnel-junction capacitor with $R_0=810$ kΩ. (For the remainder of this letter all capacitance values are normalized to area.) The junction can be modeled by a complex lossy capacitance, $C_1(\omega)-iC_2(\omega)$, in parallel with a frequency-independent tunnel junction resistor $R_0$. Since the imaginary part of the capacitance represents frequency-dependent dissipation, we can model the response as the capacitance $C_1(\omega)$ in parallel with the frequency-dependent resistance $R_p(\omega)$, which satisfies $R_p(\omega)^{-1}=R_0^{-1}+\omega C_2(\omega)$. It is straightforward to derive the relations:

$$C_1(\omega)=-\frac{\sin[\Theta(\omega)]}{\omega|Z(\omega)|}, \tag{1}$$

and

$$C_2(\omega)=\frac{\cos[\Theta(\omega)]}{\omega|Z(\omega)|}-\frac{1}{\omega R_0}, \tag{2}$$

where $Z(\omega)=|Z(\omega)|\exp[i\Theta(\omega)]$ is the complex impedance. Accordingly, independent measurements of the three quantities, $|Z(\omega)|$, $\Theta(\omega)$, and $R_0$, are sufficient to determine $C_1(\omega)$, $C_2(\omega)$, and $R_p(\omega)$.

Figure 2 shows the frequency dependence on logarithmic axes of the magnitude of the admittance $|Y(\omega)|=1/|Z(\omega)|$ for the same junction aged to six successively higher tunnel-junction resistances. Admittance is normalized to the area of the junction and the tunnel-junction resistances span the range $R_0=1360$ Ω (top curve) to $R_0=2.35$ MΩ (bottom curve). At sufficiently low frequency, the response is frequency independent ($\theta=0$) and $Y=1/AR_0$. Above a corner frequency $\omega_c\sim1/R_0C_1$ for each curve, the response is

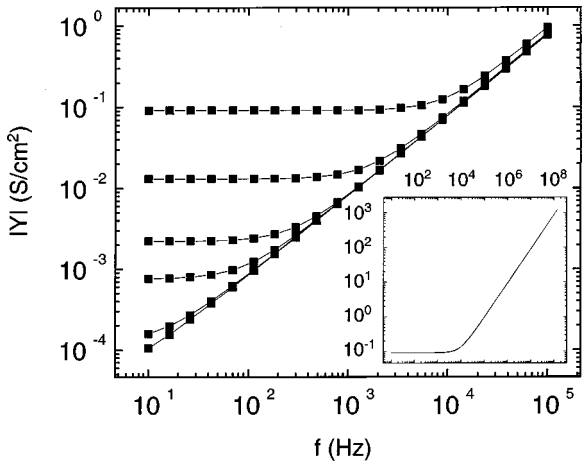


FIG. 2. Frequency dependence of the magnitude of the admittance for a tunnel junction annealed from $R_0=1360$ Ω (top curve) to $R_0=2.35$ MΩ (bottom curve). The inset shows the scaling collapse of these same data using normalized arbitrary units and $R_0$ as a scaling parameter.

primarily capacitive with $\theta\rightarrow-90°$ and $|Y(\omega)|\rightarrow\omega\sqrt{C_1(\omega)^2+C_2(\omega)^2}$. At first sight, the curves in Fig. 2 look like those of a simple RC circuit (frequency-independent capacitance) in which $Y$ would have a linear dependence on $\omega$. Closer inspection of these data and data taken on other junctions reveals, however, that the slope is neither unity nor constant.

The resistance of a tunnel junction with barrier height $\varphi$ is exponentially sensitive to the product $\varphi^{1/2}d$, whereas the capacitance is only linearly sensitive to $d$. If the additional oxidation associated with annealing is only giving rise to a larger $d$, then there will be an exponentially large increase in $R_0$ and a much smaller decrease in $|C|=\sqrt{C_1^2+C_2^2}$, as is in fact the case in Fig. 2 where the low-frequency admittance ($\propto R_0^{-1}$) decreases much faster than the high-frequency admittance ($\propto|C|$). The actual situation is more complicated since real interfaces are rough and $R_0$ reflects tunneling processes that occur with greater probability at places where the electrodes have minimum separation, whereas the capacitance depends on the average plate separation. In spite of these complications, there is a surprising simplification when the data are re-plotted as shown in the inset of Fig. 2. In this plot using normalized logarithmic axes, each of the data sets has been scaled to the topmost curve ($R_0=1.36$ kΩ) by multiplying both the abscissa and ordinate by the same constant, i.e., the $R_0$ for that curve normalized to1.36 kΩ. Minor adjustments (<5%) to the values of $R_0$ for each curve have been made. This scaling collapse onto a single curve implies the functional form $|Y(\omega)|=F(\omega R_0)/R_0$, where $F(\omega R_0)$ is a scaling function with the shape shown in the inset of Fig. 2. The phase angle $\theta$, defined by the relation $\tan(\Theta)=-\omega R_p(\omega)C_1(\omega)$ is found to scale in a similar manner. This scaling behavior points to an unexpected (and incompletely understood) simplification in categorizing the frequency response of MIM tunnel junctions.

An additional understanding of the physical processes occurring during tunnel-junction aging can be gained by presenting the complex capacitance data on a Cole–Cole plot in which $C_2(\omega)$ is plotted against $C_1(\omega)$. This dependence is shown in Fig. 3 for a subset of three junctions in which $C_1(\omega)$ and $C_2(\omega)$ have been calculated from Eqs. (1) and

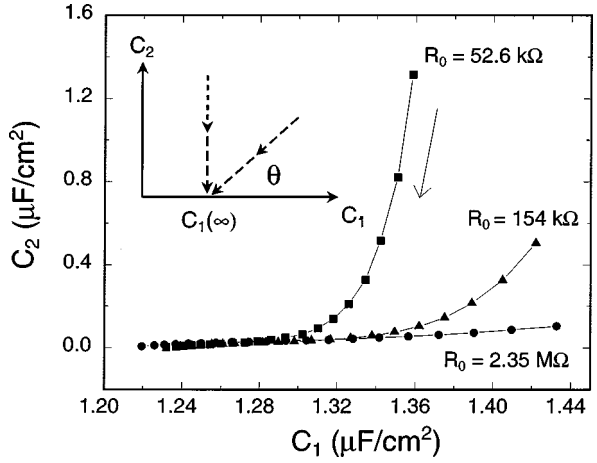


FIG. 3. Complex capacitance (Cole–Cole) plot for the same junction aged to the indicated values of dc tunnel-junction resistance. The inset schematically illustrates the response of a leaky capacitor (vertical dashed line) and a ''universal'' constant phase angle lossy capacitor (dashed line inclined at the angle $\theta$ with respect to the $C_1$ axis).

(2) using the indicated tunnel-junction resistances. The dashed arrow indicates the direction of increasing frequency. We note that all of the curves have positive curvature and there is no indication of a loss peak over the measured frequency range. As indicated by Eq. (2), at sufficiently low frequency, $|Z(\omega)|\rightarrow R_0$, and $C_2(\omega)$ must roll over to zero after first reaching a peak. Experimentally, this low-frequency region is difficult to characterize because of the long measurement times required and the sensitivity of the calculation of $C_2(\omega)$ to the small differences between $R_p(\omega)$ and $R_0$.

The high-frequency limits of two common complex capacitive responses are shown in the inset of Fig. 3. The first of these, the vertical dashed line, represents an elementary *leaky* capacitor which is modeled by a parallel combination of a frequency-independent capacitor and dc resistor. The similarity in the behavior of this elementary RC model to the tunnel-junction data occurs only at low frequency where the dependence of $C_2(\omega)$ on $C_1(\omega)$ becomes increasingly steep. The second response, shown as the dashed line inclined at the angle $\theta$ with respect to the $C_1(\omega)$ axis, represents the high-frequency response of a *lossy* capacitor, which, in contrast to a *leaky* capacitor, does not pass dc current. This constant phase angle (CPA) response has been seen in literally hundreds of materials and, since the work of Jonscher,[7] has been united under the common name of ''universal dielectric response.'' The point of this discussion is that the power-law dependence on frequency of the ''universal'' capacitance, usually attributed to glass like behavior, is *not* observed. With increasing $\omega$, $C_2$ does not extrapolate with a linear dependence to zero at a readily identified point $C_1(\infty)$ on the $C_1$ axis. Rather, $C_2$ approaches zero asymptotically with positive curvature and a constantly diminishing phase angle. We refer to this rather unusual behavior as an asymptotic phase angle (APA) response and are not aware of its existence in other dielectric systems. We cannot, however, exclude the possibility of CPA behavior at frequencies higher than $10^5$ Hz.

It is reasonable to expect that the physical processes giving rise to our observed low-frequency behavior are associated with electronic traps at the tunnel-junction interfaces. The interfaces are not uniform and contain defects, such as incompletely oxidized aluminum or impurities, which give rise to localized states with a distribution of trapping energies. The localized states hybridize with conduction electrons to form interface states, which affect the current–voltage characteristics, generate low-frequency noise, and change the capacitance.[6] The change in capacitance is proportional to the length of time a tunneling electron spends trapped at a defect site. Clearly, the presence of such states will introduce diffuse scattering and change the details of the potential variations shown in the Fig.1 inset. If we assume that the annealing or aging process described above removes a subset of these traps, then many of the trends seen in our data can be readily explained. The removal of traps certainly causes an increase in $R_0$, since for each trap removed a parallel process for elastic tunneling via a trap has been eliminated. Our observation that the dominant effect of annealing is on $C_2$ rather than $C_1$ confirms this interpretation and leads us to conclude that a removal of traps rather than a thickening of the barrier is the primary consequence of aging.

Interesting questions remain. For example, our results are, strictly speaking, independent of junction area but might be expected to be substantially different if the area is small enough to include only a few defect sites. Indeed, experiments on small-area $Al–Al_2O_3–Al$ tunnel junctions,[8,9] which exhibit Coulomb blockade effects and have lateral dimensions in the range 80–150 nm, have interface capacitance values in the range 3–6 $\mu$F/cm$^2$, substantially larger than the 1.6 $\mu$F/cm$^2$ of larger-area ($4\times10^{-4}$ cm$^2$) junctions.[3] The presumed absence of interface traps in these small junctions and the corresponding smaller drop in voltage across the interface results in a smaller $d_0$ and a larger $C_i$. An even larger interface capacitance of $\sim$35 $\mu$F/cm$^2$ has been reported for alkanethiol self-assembled monolayers used as a dielectric spacing between liquid-mercury electrodes.[10] Since mercury would be expected to have a surface that is smooth, compliant, and free of defects, this result leads us to suspect that roughness may play a critical role in determining the ac response of MIM tunnel junctions.

The authors would like to acknowledge useful discussions with Glen Alers. This work was supported by NSF Grant No. DMR 9705224.

[1] C. A. Mead, Phys. Rev. Lett. **6**, 545 (1961).
[2] A. Goswami and A. P. Goswami, Thin Solid Films **16**, 175 (1973).
[3] A. F. Hebard, S. A. Ajuria, and R. H. Eick, Appl. Phys. Lett. **51**, 1349 (1987).
[4] S. Zafar, R. E. Jones, P. Chu, B. White, B. Jiang, D. Taylor, P. Zurcher, and S. Gillepsie, Appl. Phys. Lett. **72**, 2820 (1998).
[5] J. Krupski, Phys. Status Solidi B **157**, 199 (1990).
[6] J. Halbritter, J. Appl. Phys. **58**, 1320 (1985).
[7] A. K. Jonscher, Nature (London) **267**, 673 (1977).
[8] P. Joyez, D. Esteve, and M. H. Devoret, Phys. Rev. Lett. **80**, 1956 (1998).
[9] R. J. Schoelkopf, P. Wahlgren, A. A. Kozhevnikov, P. Delsing, and D. E. Prober, Science **280**, 1238 (1998).
[10] M. A. Rampi, O. J. A. Schueller, and G. M. Whitesides, Appl. Phys. Lett. **72**, 1781 (1998).